Draft version August 4, 2016
Preprint typeset using LaTeX style emulateapj v. 5/2/11

arXiv:1608.01242v1 [astro-ph.SR] 3 Aug 2016

NEW ORBITS BASED ON SPECKLE INTERFEROMETRY AT SOAR[1]

Andrei Tokovinin
Cerro Tololo Inter-American Observatory, Casilla 603, La Serena, Chile
Draft version August 4, 2016

ABSTRACT

Orbits of 55 visual binary stars are computed using recent speckle interferometry data from the SOAR telescope: 33 first-time orbits and 22 revisions of previous orbit calculations. The orbital periods range from 1.4 to 370 years, the quality of orbits ranges from definitive to preliminary and tentative. Most binaries consist of low-mass dwarfs and have short periods (median period 31 years). The dynamical parallaxes and masses are evaluated and compared to the *Hipparcos* parallaxes. Using differential speckle photometry, binary components are placed on the color-magnitude diagram.

1. INTRODUCTION

This paper presents new or updated orbits for 55 binary systems or subsystems. It is based on speckle interferometric measurements made at the 4.1-m Southern Astrophyisical Research (SOAR) telescope (Tokovinin et al. 2010a,b; Tokovinin 2012; Tokovinin et al. 2014, 2015, 2016) combined with archival data collected in the Washington Double Star Catalog, WDS (Mason et al. 2001). It continues previous work on binary orbits resulting from the SOAR speckle program.

The Sixth Catalog of Visual Binary Orbits, VB6[2] (Hartkopf, Mason & Worley 2001), presently contains orbital elements of more than 2600 pairs. Knowledge of binary orbits is needed in various areas such as: (i) measurement of stellar masses (especially for stars of very low or high mass, unusual chemical composition or at various evolutionary stages); (ii) statistics of orbital elements in relation to mechanisms of binary formation and evolution; (iii) accurate models of stellar motion for astrometry; (iv) binary systems of special interest, for example exohosts or young binaries with circumstellar material. The latter class is poorly defined, given that a common "uninteresting" binary may suddenly become important in the light of new discoveries, e.g. the visual triple star HD 131399 hosting an unusual planet (Wagner et al. 2016). Accurate parallaxes soon to be available from *Gaia* will greatly enhance the value of binary orbits for calibration of stellar masses. During five years of this mission, only portions of long binary periods will be covered, making the ground-based monitoring an essential complement. These arguments indicate that the work on binary orbits is part of the astronomical infrastructure and has its own value.

Most binaries studied here consist of late-type dwarfs in the solar neighborhood, including close pairs first resolved by *Hipparcos*. These pairs have orbital periods measured in years and decades, while wider classical visual binaries have periods of a few centuries or millenia. Efforts to monitor the motion of these fast binaries by speckle interferometry have been made by Balega et al. (2006), Horch et al. (2015), and others mostly on the northern sky. The SOAR data on their southern counterparts reveal a fast motion and the lack of coverage after the *Hipparcos* discovery in 1991. First, still preliminary orbits of several such pairs are presented here.

Another class of preliminary orbits have long periods and incomplete orbit coverage, so typical for visual orbits. Unlike spectroscopists who accumulate data for one or several orbital revolutions before publishing the orbit, the visual binary community has a tradition of sharing the observations, because the time needed for an orbit calculation may exceed the human life span. The downside of this tradition is publication of premature orbits and frequent, sometimes poorly justified orbit revisions. One of the reasons for publishing here uncertain first-time orbits is the need to understand the orbital motion and to plan further observations for their improvement.

Compared to visual micrometer measures, speckle interferometry has a much improved accuracy (the SOAR data have random and systematic errors of a few mas). Some classical binaries discovered and measured at the limit of visual techniques have now reliable and accurate orbits based on speckle interferometry. Large resolving power of the 4.1-m SOAR telescope allows to map previously inaccessible portions of their orbits near periastron. This is particularly important for difficult orbits with high eccentricity or oriented edge-on. Such orbits are under-represented in the VB6 and hence distort the statistics.

Traditionally, visual binary orbits were mostly computed by the observers themselves who had a deep understanding of the underlying data and its reliability. Speckle interferometry is more reliable than micrometer measures; however, measures of close or very unequal pairs near the limit of the technique can also be unreliable or distorted by instrumental artifacts. Access to the original SOAR data and the possibility to reprocess doubtful measures distinguishes this work from orbit calculation made by others.

2. ORBITAL ELEMENTS

Orbital elements and their errors are determined by least-squares fitting using the IDL code `ORBIT`.[3] When no prior orbit is available, the initial approximation is

atokovinin@ctio.noao.edu
[1] Based on observations obtained at the Southern Astrophysical Research (SOAR) telescope.
[2] `http://www.usno.navy.mil/USNO/astrometry/optical-IR-prod/wds/orb6`
[3] `http://www.ctio.noao.edu/~{}atokovin/orbit/index.html`

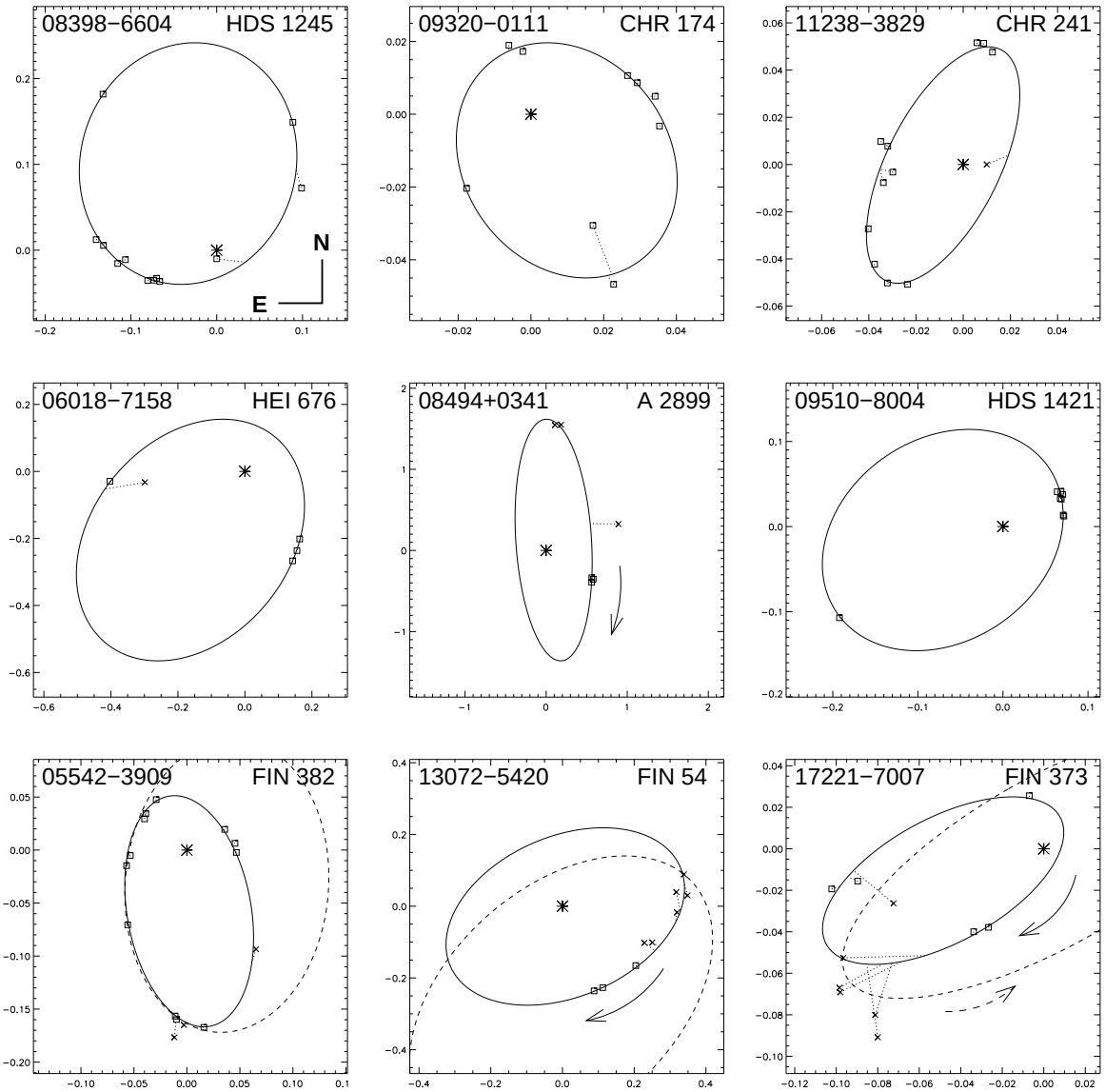

Figure 1. Plots of selected orbits. Top row: reliable new orbits, middle row: preliminary new orbits, bottom row: orbit revisions (old orbits in dashed line). In each plot, the primary component is located at the coordinate origin and the scale is in arcseconds. Squares and crosses denote speckle and visual measurements, respectively. They are connected by dotted lines to the ephemeris positions on the orbital ellipse (full line).

chosen interactively, considering the observed motion of each pair. This step is non-trivial because position angles are determined by speckle interferometry only modulo 180°, allowing quadrant "flips", the orbit coverage often has large gaps, and some measurements are simply erroneous. Sometimes the same data can be represented by several very different orbits.

The least-squares method implies that the measurement errors are known and normally distributed; in such case the optimum weights are inversely proportional to the squares of the errors. Visual measurements do not match this model, having random and/or systematic errors that are difficult to quantify. The errors of speckle interferometry behave better, but depend on the instrument, telescope aperture, magnitude difference, wavelength, data quality, etc., so there are no simple prescriptions for their evaluation. Here the errors are assigned subjectively based on these considerations and are corrected iteratively by assigning larger errors (hence smaller weights) to the outliers. The result is checked by computing the χ^2/N metric, where N is the number of degrees of freedom. In the ideal case, $\chi^2/N \sim 1$. The same error in the radial and tangential directions is adopted for each observation. This is true for speckle interferometry, while the known tendency of visual observers to measure angles more accurately than separations is ignored here, considering low weight of the visual data. For many pairs observed at SOAR, the rms residuals from the orbits are on the order of 1 mas. The weighting scheme adopted in the VB6 does not fully account for the high accuracy of SOAR data; as a result, some recent orbits (e.g. Tokovinin et al. 2015) are "pulled away" by inaccurate old measures and leave systematic residuals to the SOAR data.

As mentioned above, for some binaries the scarce available observations do not fully constrain their orbital el-

ements and are compatible with a wide range of orbits. In such cases, the mass sum calculated using the HIP2 parallax (van Leeuwen 2007) provides a guidance on selecting the most plausible orbit. Some orbital elements can be fixed while fitting the remaining elements, so that the resulting mass sum takes a reasonable value. This approach does not work for binaries with unknown or small parallax.

Table 1 lists the orbital elements and their errors in common notation (P – orbital period, T_0 – epoch of periastron, e – eccentricity, a – semimajor axis, Ω – position angle of the node for the equinox J2000.0, ω – argument of periastron, i – inclination). The first column gives the WDS code of the binary and, in the following line, its *Hipparcos* number when available. The system identifier adopted in the WDS ("discoverer code") is given in the second column. For each pair, the first line contains orbital elements, while the following line gives their formal errors. The errors are omitted for some preliminary orbits of grade 5 where they have no sense. Provisional grades are assigned based on the principles described in the VB6, where grades 4 and 5 mean preliminary orbits and grade 1 are definitive and accurate orbits. The last column contains references to previously computed orbits, when available.

Figure 1 gives samples of orbital plots, illustrating their different quality. Its top row shows three first-time, but well defined orbits. The second row shows new preliminary orbits that risk substantial revisions in the future, mostly because the coverage is still insufficient. Drastic revisions of previous orbits are shown in the bottom row.

Individual observations and residuals are listed in Table 2, available in full electronically. It contains still unpublished measures made at SOAR in 2016, while some published SOAR measures were reprocessed. Its first column identifies the binary by its WDS code. Then follow the time of observation T in Besselian years, position angle θ for the time of observation (correction for precession is done internally during orbit calculation), separation ρ in arcseconds, and measurement error σ. Unrealistically large errors are assigned to the discarded observations, so that they have no influence on the fitted elements but are still kept in the Table. The last two columns of Table 2 contain the residuals O−C in angle and separation.

Table 3 provides additional information, namely the the spectral type as given in *Hipparcos* or SIMBAD and the HIP2 parallax $\pi_{\rm HIP2}$, to be compared to the dynamical parallax $\pi_{\rm dyn}$ in the next column. The latter is evaluated by the Baize-Romani method, applicable when binary components follow the standard main-sequence relation between mass and absolute magnitude. Taking the initial mass sum $\mathcal{M} = 2\mathcal{M}_\odot$, I compute the dynamical parallax $\pi_{\rm dyn} = a\mathcal{M}^{-1/3}P^{-2/3}$, use it to evaluate the absolute V magnitudes of both components, and estimate their masses $\mathcal{M}_1$ and $\mathcal{M}_2$ by means of the standard relation by Henry & McCarthy (1993), valid for $\mathcal{M} < 2\mathcal{M}_\odot$ and extrapolated to larger masses in a few cases. The new mass sum leads to the new value of $\pi_{\rm dyn}$, and the iterations converge rapidly. The components' masses $\mathcal{M}_1$ and $\mathcal{M}_2$ obtained in this procedure are listed in the columns (6) and (7) of Table 3. Asterisks mark the dynamical parallaxes derived from reliable orbits of grade 3 or better. Figure 2 compares the dynamical and

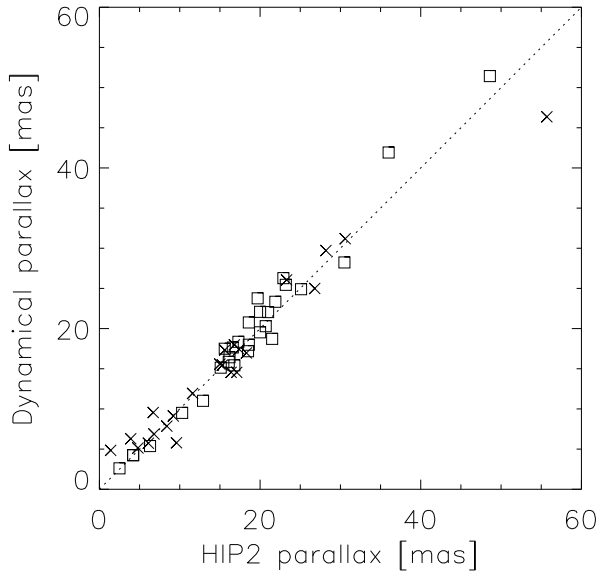

Figure 2. Comparison between the dynamical and *Hipparcos* parallaxes. Binaries with orbits of grade 3 or better are plotted by squares, the remaining binaries by crosses.

Hipparcos parallaxes.

The combined V magnitude and $V-I_C$ color index in columns (8) and (9) are taken mostly from the *Hipparcos* catalog. For HIP 83716B and 87914B, the combined magnitudes refer to the secondary subsystems, while $V-I_C = 1.0$ mag is assumed to match the estimated spectral type K0V of both pairs. The last four columns of Table 3 provide differential photometry resulting from the SOAR speckle interferometry, where the filters y and I have central wavelengths and bandwidths of 543/22 and 788/132 nm, respectively. The Δy and ΔI are average values, while $\sigma_{\Delta y}$ and $\sigma_{\Delta I}$ stand for the rms scatter of magnitude difference in each filter if measured several times, indicating internal consistency of the differential photometry. For some pairs this scatter is as good as 0.1 mag, but it can be up to ∼0.5 mag. Speckle differential photometry is unreliable for very close pairs at or below the diffraction limit. For faint or wide binaries, Δm can be systematically overestimated. Despite these caveats, speckle interferometry at SOAR is the only source of differential photometry for some close binaries.

When both Δy and ΔI are measured, the empirical linear relation $\Delta I \approx 0.7\Delta y$ holds, allowing to estimate differential magnitudes in both filters even when measurements in only one filter are available. It is also reasonable to assume that $\Delta V \approx \Delta y$ and $\Delta I_C \approx \Delta I$. Therefore, magnitudes and colors of each binary component can be estimated using combined and differential photometry.

Figure 3 shows the $(M_V, V-I_C)$ color-magnitude diagram (CMD) where only binaries with $\pi_{\rm HIP2} > 4$ mas are plotted. For reference, the 1-Gyr isochrones from Dotter et al. (2008) and Baraffe et al. (2015) are shown.

3. NOTES ON INDIVIDUAL BINARIES

Brief comments on some binaries are provided in this Section. The acronym RV stands for radial velocity.

04180−3826. HDS 546 is a typical case of a *Hipparcos* binary that has not been observed after its discovery in 1991. It has made one full revolution since, and the short arc observed at SOAR shows a rapid motion. This is a

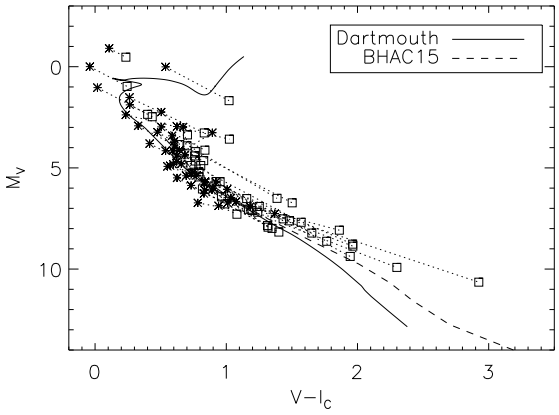

Figure 3. Color-magnitude diagram. The primary and secondary components of each pair are plotted as asterisks and squares, respectively, and connected by dotted lines. The full line is the Dartmouth isochrone (Dotter et al. 2008), the dashed line is the BHAC15 (Baraffe et al. 2015) isochrone, both for 1 Gyr age and solar metallicity.

pair of K2V chromospherically active dwarfs.

05229-4219. TOK 93 Aa,Ab was first resolved in 2011 at Gemini-S (Tokovinin et al. 2012). It has a variable RV and astrometric acceleration. Some observations have been re-processed. The faint star B at 14″ is physical.

05542-2909. The orbit of FIN 382 with $P = 20.16$ yr given in (Tokovinin et al. 2015) is wrong (Figure 1), the true period is 10 yr. The revised orbit has a very high quality, with the rms residuals of 3.6 and 1.8 mas in two coordinates.

08369−7857. KOH 79 is a young variable star EG Cha in the η Cha association. Two preliminary orbits proposed by Koehler & Petr-Gotzens (2002) are now replaced by one non-ambiguous, though still preliminary, orbit. The dynamical parallax of 11.5 mas matches the known distance to this association and may eventually help to measure it better.

09149+0427. HEI 350 is a nearby red dwarf pair GJ 390 (the spectral type of the primary is K4V). Despite the large Δm, the two first micromemeter measures by W. Heintz in 1987 and 1988 have contradictory quadrants, and both do not agree well with the accurate measures available since 2003. The pair has not been resolved by *Hiparcos*, presumably because of the large Δm. The orbit is only loosely constrained. The binary might be young and belong to the Castor moving group. Its secondary with $V - I_C = 3.15$ mag is located above the main sequence in Figure 3; the large magnitude difference $\Delta V = 4.0$ mag has been confirmed in 2016.4.

09275-5806. The orbit of CHR 240 published in (Tokovinin et al. 2015) is substantially revised, with a new period of 1.42 yr instead of 2.62 yr. This very close pair is often under the diffraction limit of SOAR.

09466−4966. Our relative photometry implies that $\Delta I > \Delta y$, i.e. the secondary is bluer than the primary. The G5IV primary is evolved; it is located in the subgiant branch of the CMD. The *Hipparcos* photometry $\Delta Hp = 1.24$ mag is suspect because in 1991 the pair was very close, 0.″15.

09510-8004. HDS 1421 (B8IV) belongs to the Sco-Cen association; the dynamical parallax is 6.4 mas. The orbit is still preliminary, but its curvature is well defined.

11102-1122. HDS 1590 (HD 97038) is a double-lined spectroscopic binary (D. Latham, 2012, private communication). Its corrected orbit is now well defined after coverage of the periastron.

13072−5420. Despite the drastic revision of the previous orbit, the elements of FIN 54 remain tentative, given that only a small arc is covered (Figure 1). One of the components is an eclipsing binary V949 Cen. The dynamical parallax is 4.8 mas, substantially larger than 1.3 mas measured by *Hipparcos*.

13377−2337. Two orbits of RST 2856 (BD−22° 3633) by Heintz (1997) with periods of 110 yr and 51.5 yr are now replaced by the new, but still tentative orbit with $P = 122$ yr. It is based on two HRCam measures and a handful of visual micrometer measures. The $\Delta y = 2.1$ mag is derived from the very noisy data and is likely wrong; the pair has not been resolved by *Hipparcos* despite its 0.″3 separation. The dynamical parallax is 12.3 mas, the matching spectral type of the primary is G5V.

13598−0333. This star HR 5278 (F6V) possibly contains a debris disk. A slight revision of the previous orbit by Horch et al. (2011) leaves very well defined elements. Both components are at about 1.5 mag above the main sequence, while the mass sum is slightly larger than expected. The stars could have evolved off the main sequence or are still contracting.

14383−4954. A drastic revision of the orbit by Zirm (2014) changes the period of FIN 371 from 27.6 yr to 50.7 yr.

14453−3609. The first tentative orbit for I 528, with a poor coverage and doubtful visual measures, is suggested. The formal errors of the elements are misleadingly small. The component C is at 4.″5. The dynamic parallax is 5.3 mas, and the binary may belong to the Sco-Cen association.

14589+0636. WSI 81 (HIP 73314) is on the California planet search program (Isaacson & Fischer 2010). The new orbit is well defined and leads to the mass sum of 2.2 $\mathcal{M}_\odot$, while the dynamical parallax corresponds to 1.7 $\mathcal{M}_\odot$. Both components are located on the main sequence.

15035−4035. The revision of the orbit by Heintz (1981) for I 1262 nearly doubles its period, from 134 to 251 yr, but the orbit still remains preliminary and poorly constrained. The binary belongs to the Sco-Cen association, its dynamic parallax is 5.7 mas.

15042−1530. The new edge-on ($i = 89°$) orbit of RST 3906 is very different from the previous one by Heintz (1981) with $i = 129°$. The new orbit fits the speckle data well but implies that many micrometer measures of this pair are totally wrong (possibly observers confused it with another pair?). The pair was unresolved at SOAR on 2016.14 in agreement with the new orbit.

15282−0921. This nearby K2V star GJ 586 is a spectroscopic binary with a record-high eccentricity of $e = 0.976$. Precise RVs from Strassmeier et al. (2013) constrain all spectroscopic elements very tightly, leaving for adjustment only the "visual" elements a, Ω, and i. The orbital parallax is 52.5 ± 6.2 mas, the orbital masses are 0.86 ± 0.11 and 0.58 ± 0.08 $\mathcal{M}_\odot$.

15290−2852. BU 1114 is a nearby dwarf with a physical tertiary component C at 9.″6. Some published non-resolutions of AB at SOAR refer in fact to this compo-

nent C, pointed erroneously instead of AB. The edge-on orbit is preliminary and yields the mass sum of 2.0 $\mathcal{M}_\odot$, less than 2.9 $\mathcal{M}_\odot$ estimated from the luminosity.

15317+0053. TOK 48 (HIP 76031, HD 138369) is a single-lined spectroscopic binary with a period of 619.3 days (Griffin 2013). Resolved measures from SOAR are combined with the RVs of the primary component in the orbital fit. However, the solution converges to $i \approx 180°$, contradicting the observed RV variation. Therefore, in the combined speckle-spectroscopic orbit the inclination was fixed at 150°. The differential photometry $\Delta y = 1.6$ mag and $\Delta I = 1.25$ mag leaves no doubt that the spectrum should contain double lines. However, Griffin could no find them, despite dedicated effort. His hypothesis that the secondary component is a close binary is not supported by the speckle photometry, but the secondary could have a fast axial rotation, reducing the depth of its lines in the blended spectrum. Both components are located on the main sequence.

15332−2429. CHR 232 Aa,Ab (HR 5765) is an A7V chemically peculiar binary (Abt & Morrell 1995) with a new well-constrained 16.5-yr orbit (rms residuals 1 mas). A very similar orbit has just been published by Docobo et al. (2016). It has made more than one full revolution since its discovery in 1996.18. The visual companion B at 9.″2 is also a resolved close binary SEE 238 BC with a 60.4-yr orbit; its observation with HRCam in 2008.54 in fact refers to the Aa,Ab pair. The two subsystems Aa,Ab and BC in this 2+2 quadruple are not co-planar. The dynamical parallaxes of Aa,Ab and BC are 9.4 and 10.3 mas, respectively, while the HIP2 parallax is 10.4 mas. The component Ab is located above the main sequence in the CMD.

15348−2808. The first preliminary 26-yr orbit of TOK 49 Aa,Ab is computed. The outer binary RST 1847 AB has a separation of 1″.

15548−6554. The first orbit of the nearby red dwarf binary NZO 65 (G2V) is well constrained. Its components are on the main sequence.

16544−3806. This is a dramatic revision of the previous orbit of HDS 2392 by Tokovinin et al. (2015).

17018−5108. The orbit of I 1306 by Olevic & Cvetkovic (2004) with $P = 62.3$ yr is revised to $P = 194$ yr and still remains preliminary; only a half of it is covered in almost a century of observation. This is a bright star HR 6312, A9III. The mass sum of 1.0 $\mathcal{M}_\odot$ does not match the spectral type, throwing suspicion on the HIP2 parallax of 9.6 mas (the dynamical parallax is 5.8 mas).

17066+0039. After a slight correction, the orbit of the subsystem Ba,Bb with $P = 6.34$ yr is now well constrained. The outer pair BU 823 AB has a poorly defined 532-yr orbit. Coplanarity between the inner and outer orbits is not excluded.

17221−7007. A drastic revision of the orbit of FIN 373 (HR 6411, *i* Aps, B8/9V). Compared to the orbit by Docobo & Andrade (2013), even the direction of the rotation has changed from prograde to retrograde, see Figure 1. The published SOAR measure in 2009.26 was wrong and corresponded to the image doubling caused by telescope vibration; it has been reprocessed. The rms residuals to the new orbit are 1.8 mas, and it is now well defined.

17575−5740. The first 9-yr orbit of the subsystem Ba,Bb is well constrained. The outer pair AB has a separation of 2.″5 and no orbit so far.

17584+0428. KUI 84 (GJ 9609, K8) is a nearby close triple system where the secondary component of the 14.7-yr visual binary contains a 34.5-day spectroscopic subsystem (Tokovinin 1994). The secondary component is located above the main sequence in the CMD, as expected. Deviations of the speckle measures from the latest visual orbit by Docobo & Ling (2005) prompted its slight revision here. RVs were used together with the speckle measures, leading to a very well-defined orbit. The HIP2 parallax of 22.9 mas corresponds to the mass sum of 2.0 $\mathcal{M}_\odot$, while the orbital parallax of 26.3 mas and the mass sum of 1.3 $\mathcal{M}_\odot$ are a better match to the masses estimated by Tokovinin (1994).

18150−5018. The first orbit of I 429 (HD 166839, A0V) looks reasonable, but then the discovery measure by Innes in 1902.5 at a separation of 0.″5 must be totally wrong. This and other measures made before 1929 were ignored in the orbit calculation. Presently the pair is approaching periastron.

18368−2617. The new orbit of RST 2187 AB looks good, but corresponds to the mass sum of 1.4 $\mathcal{M}_\odot$. A revision of the HIP2 parallax from 21.5±1.7 mas to 19 mas is needed to increase the mass sum of this pair of nearly equal G3V stars to 2 $\mathcal{M}_\odot$. The tertiary component C at 12.″6 is physical.

18480−1009. HDS 2665 is a nearby K2V dwarf. The primary component is located on the main sequence, while the secondary is above it. The mass sum of 2.0 $\mathcal{M}_\odot$ is somewhat larger than expected, so there may be inner subsystems.

19581−4808. Some observations of the nearby G0V dwarf binary HDS 2842 were reprocessed for a minor revision of its previous 32-yr orbit, now definitive.

20217−3637. HDS 2908 (HD 193464, F8V) is another nearby dwarf binary. Double lines were noticed, but there is no spectroscopic orbit in the literature. The $\Delta y = 0.49$ mag is based on two well-resolved observations and is more reliable than $\Delta Hp = 0.21$ mag.

22116−3428. The 66-yr first orbit of CHR 230 Aa,Ab (K1/K2III) is well defined. The outer binary AB has a separation of 0.″9. The large eccentricity $e = 0.93$ of Aa,Ab could be caused by the Kozai-Lidov cycles. Both components are located on the giant branch in the CMD (Figure 3).

4. SUMMARY

New and updated orbits presented here make an incremental improvement of the VB6 content and thus contribute, albeit in a small way, to the observational foundations of astronomy. Some of these binaries are interesting because they are members of multiple systems with three or more components, are young, lead to the useful measurements of masses, or for other reasons.

This work used the SIMBAD service operated by Centre des Données Stellaires (Strasbourg, France), bibliographic references from the Astrophysics Data System maintained by SAO/NASA, and the Washington Double Star Catalog maintained at USNO.

Facilities: SOAR.

REFERENCES

Abt, H. A. & Morrell, N. I. 1995, ApJS, 99, 135
Baize, P. 1989, AAS, 78, 125
Balega, I. I., Balega, Y. Y., Hofmann, K.-H. et al. 2006, A&A, 448, 703
Baraffe, I., Homeier, D., Allard, F. & Chabrier, G. 2015, A&A, 577, 42 (BHAC15)
Docobo, J. A. & Ling, J. F. 2005, IAUDS, 157, 1
Docobo, J. A. & Andrade, M. 2013, MNRAS, 428, 321
Docobo, J. A., Gomez, J. & Campo, P. P. 2016, IAUDS, 189, 1
Dotter, A., Chaboyer, B., Jevremović, D. et al. 2008, ApJS, 178, 89
Griffin, R. F. 2013, Obs. 133, 1
Hartkopf, W. I., Mason, B. D. & Worley, C. E. 2001, AJ, 122, 3472 (VB6)
Hartkopf, W. I. & Mason, B. D. 2011, IAUDS, 175, 1
Heintz, W. D. 1981, ApJS, 45, 559
Heintz, W. D. & Cantor, B. 1992, Obs, 112, 286
Heintz, W. D. 1996, ApJS, 105, 475
Heintz, W. D. 1997, ApJS, 111, 335
Henry, T. J. & McCarthy, D. W. 1993, AJ, 106, 773
Horch, E. P., van Altena, W. F., Howell, S. B. et al. 2011, AJ, 141, 180
Horch, E. P., van Belle, G. T., Davidson, J. W., Jr. et al. 2015, AJ, 150, 151
Isaacson, H. & Fischer, D. 2010, ApJ, 725, 875
Koehler, R. & Petr-Gotzens, M. G. 2002, AJ, 124, 2899
Mason, B. D., Wycoff, G. L., Hartkopf, W. I. et al. 2001, AJ, 122, 3466 (WDS)
Olevic, D. & Cvetkovic, Z. 2004, A&A, 415, 259
Strassmeier, K. G., Weber, M., & Granzer, T. 2013, A&A, 559, 17
Tokovinin, A. A. 1994, AstL, 20, 309
Tokovinin, A., Mason, B. D., & Hartkopf, W. I. 2010a, AJ, 139, 743
Tokovinin, A. Cantarutti, R., Tighe, R. et al. 2010b, PASP, 122, 1483
Tokovinin, A. 2012, AJ, 144, 56
Tokovinin, A., Hartung, M., Hayward, Th. L., & Makarov, V. V. 2012, AJ, 144, 7
Tokovinin, A., Mason, B. D., & Hartkopf, W. I. 2014, AJ, 147, 123
Tokovinin, A., Mason, B. D., & Hartkopf, W. I. et al. 2015, AJ, 150, 50 (SOAR14)
Tokovinin, A., Mason, B. D., & Hartkopf, W. I. et al. 2016, AJ, 153, 151
van den Bos, W. H. 1961, CiUO, 120, 380
van Leeuwen, F. 2007, A&A, 474, 653 (HIP2)
Wagner, K., Apai, D., Kasper, M. et al. 2016, Science, 10.1126/science.aaf9671
Zirm, H. 2014, IAUDS, 182, 1

Table 1
Orbital Elements

WDS HIP	Discoverer Designation	P (yr)	T_0 (yr)	e	a ($''$)	Ω (°)	ω (°)	i (°)	Gr	Orbit Reference
04180−3826	HDS 546	22.674	2014.439	0.422	0.2333	53.2	211.1	110.6	4	New[a]
20048		±0.218	±0.087	±0.028	±0.0052	±2.2	±5.2	fixed		
05229−4219	TOK 93 Aa,Ab	5.680	2013.511	0.481	0.0594	225.6	92.6	59.6	3	New
25148		±0.270	±0.088	±0.041	±0.0033	±4.1	±3.4	±3.0		
05542−2909	FIN 382	10.070	2015.397	0.537	0.1117	194.8	200.1	127.7	1	Tok2015c[b]
27901		±0.036	±0.018	±0.004	±0.0014	±1.2	±1.6	±1.0		
06018−7158	HEI 676	102.0	2006.39	0.657	0.3988	301.9	340.0	169.0	5	New[a,b]
28573		±12.5	±0.18	±0.035	±0.0237	±1.2	fixed	fixed		
06032+1922	HDS 823 Aa,Ab	100	2044.6	0.93	0.449	51.5	80.2	95.9	5	New
28671		...	...	...	...	...	...	...		
08369−7857	KOH 79 AB	77.1	1996.4	0.291	0.2441	182.0	320.7	106.2	4	Koh2002
...		±8.9	±1.5	±0.052	±0.0207	±1.3	±11.3	±1.5		
08398−6604	HDS 1245	33.84	2013.175	0.781	0.2118	299.6	97.3	129.5	2	New[b]
42496		±0.90	±0.055	±0.013	±0.0059	±1.8	±1.7	±2.6		
08494+0341	A 2899	300	2123	0.231	1.53	4.0	250.4	107.8	5	New[a,b]
43304		fixed	±51	±0.059	±0.19	±5.1	±39.9	±3.6		
09149+0427	HEI 350	62.68	1984.83	0.20	0.810	102.3	263.6	136.0	5	Tok2015c[a]
45383		±2.88	±1.60	fixed	±0.037	±2.1	±10.6	±3.0		
09186+2049	HO 43	358.6	1941.2	0.40	0.610	80.0	214.9	131.6	4	Baz1989a
45671		±9.4	±2.5	fixed	±0.013	±3.6	±6.7	±2.3		
09275−5806	CHR 240	1.421	2015.376	0.391	0.0324	259.2	141.3	130.0	2	Tok2015c
46388		±0.007	±0.027	±0.038	±0.0009	±5.3	±8.6	fixed		
09320−0111	CHR 174	6.09	2015.06	0.471	0.0342	29.6	351.1	159.4	2	New[b]
46776		±0.14	±0.04	±0.019	±0.0022	±32.5	±30.6	±12.1		
09466−4955	HDS 1414	60	2018.67	0.80	0.144	291.3	243.1	62.8	5	New[a]
47969		fixed	±2.76	±0.35	±0.128	±10.6	±30.9	±34.1		
09510−8004	HDS 1421	63.52	2015.24	0.50	0.1583	142.3	135.2	34.5	4	New[a,b]
48320		±5.68	±0.37	fixed	±0.0057	±15.8	±20.9	±7.0		
10112−3245	HDS 1469	30.54	2015.323	0.636	0.1482	206.9	156.0	134.8	4	New[a]
49883		±3.92	±0.474	fixed	±0.0235	±11.2	±17.6	±15.6		
11102−1122	HDS 1590	20.61	1995.616	0.783	0.1613	254.7	74.6	120.7	3	Tok2015c
54580		±0.43	±0.424	±0.009	±0.0044	±1.6	±0.8	±1.0		
11238−3829	CHR 241	3.559	2013.264	0.322	0.0576	154.2	257.8	114.7	3	New
55628		±0.022	±0.078	±0.029	±0.0014	±2.1	±3.7	±1.8		
11425+2355	COU 390	92.75	2007.86	0.786	0.5498	231.4	100.9	43.6	3	New
57112		±5.57	±0.28	±0.014	±0.0168	±3.2	±2.7	±3.2		
11525−1408	HDS 1676	16.71	1999.60	0.681	0.1474	324.6	307.5	48.2	3	Tok2014a
57894		±0.42	±0.42	±0.010	±0.0030	±2.0	±2.9	±1.7		
13072−5420	FIN 54	373.7	2189.08	0.01	0.3516	113.3	79.7	135.3	5	Hrt2011d[a,b]
64025		...	...	...	...	...	...	...		
13081−7719	HDS 1839	17.44	2014.11	0.168	0.2007	349.2	320.5	120.5	4	New[a]
64091		±1.03	±0.84	±0.104	±0.0124	±5.4	±19.0	±2.5		
13306−4238	HDS 1891	12.51	2014.76	0.192	0.185	99.9	273.2	162.6	4	New[a]
65906		±0.05	±1.38	±0.046	±0.027	±103.7	±157.7	±27.1		
13377−2337	RST 2856	122	2038.6	0.55	0.352	108.7	290.2	81.9	5	Hei1997
...		...	...	...	...	...	...	...		
13598−0333	HDS 1962	9.496	2008.139	0.374	0.0734	205.6	49.5	49.9	3	Hor2011b
68380		±0.071	±0.060	±0.032	±0.0029	±3.7	±2.7	±3.2		
14020−2108	WSI 79	22.41	2015.258	0.735	0.1967	137.2	146.6	140.5	3	Tok2015c
68552		±2.00	±0.022	±0.015	±0.0067	±3.1	±5.0	±2.8		
14383−4954	FIN 371	51.13	2015.39	0.205	0.0998	234.4	38.9	109.1	3	Zir2014a
71577		±3.79	±1.50	±0.028	±0.0041	±1.7	±13.6	±1.5		
14453−3609	I 528 AB	28.92	2008.87	0.45	0.0748	88.8	276.4	56.2	5	New[a]
72140		±0.93	±1.11	fixed	±0.0065	±7.2	±5.6	±5.1		
14589+0636	WSI 81	9.364	2006.981	0.145	0.1344	65.0	279.1	130.5	3	New
73314		±0.049	±0.086	±0.008	±0.0015	±1.7	±4.5	±1.1		
15035−4035	I 1262	235	1920.6	0.257	0.3122	33.6	189.6	52.6	5	Hei1996a
73667		...	...	...	...	...	...	...		
15042−1530	RST 3906	53.897	2018.396	0.740	0.1570	154.5	3.7	89.4	4	Hei1981a
73724		±15.772	±3.868	±0.337	±0.0278	±1.3	±32.1	±1.5		
15251−2340	RST 2957	53.52	2020.795	0.850	0.2762	96.4	302.0	86.0	4	New
75478		±6.57	±0.722	±0.086	±0.0076	±1.3	fixed	±0.6		
15282−0921	BAG 25 Aa,Ab	2.43623	2007.2603	0.976	0.1074	272.8	255.6	55.4	2	New
75722		fixed	fixed	fixed	±0.0081	±2.1	fixed	±3.6		
15290−2852	BU 1114 AB	205	2047.16	0.498	0.7219	138.3	359.5	90.6	4	New
75790		fixed	±4.45	±0.045	±0.0272	±0.5	±5.4	±0.3		
15317+0053	TOK 48	1.713	2016.470	0.435	0.0427	161.9	45.8	150.0	3	New
76031		±0.002	±0.010	±0.017	±0.0010	±2.1	±2.3	fixed		
15332−2429	CHR 232 Aa,Ab	16.468	2011.536	0.419	0.0933	10.4	321.6	123.9	2	New
76143		±0.194	±0.064	±0.009	±0.0019	±1.9	±2.6	±0.9		
15348−2808	TOK 49 Aa,Ab	26.27	2006.28	0.342	0.1814	344.1	131.9	56.0	5	New[a]
76275		...	...	...	...	...	...	...		
15548−6554	NZO 65	120.60	2009.88	0.464	0.6831	122.2	219.0	85.7	3	New
77921		±2.18	±0.11	±0.010	±0.0085	±0.4	fixed	±0.2		

Table 1 — *Continued*

WDS HIP	Discoverer Designation	P (yr)	T_0 (yr)	e	a ($''$)	Ω (°)	ω (°)	i (°)	Gr	Orbit Reference
16544−3806	HDS 2392	26.48	2009.459	0.50	0.1858	101.3	154.8	134.7	4	Tok2015c
82709		±0.67	±0.086	fixed	±0.0045	±3.2	±2.8	±2.0		
17018−5108	I 1306	193.7	1989.59	0.187	0.317	12.8	149.0	84.6	5	Ole2004b
83321		...	...	...	...	...	...	...		
17066+0039	TOK 52 Ba,Bb	6.339	2012.979	0.386	0.0725	15.9	179.2	34.0	2	Tok2014a
83716		±0.146	±0.076	±0.023	±0.0027	±10.7	±13.6	±5.5		
17221−7007	FIN 373	56.90	2011.48	0.839	0.0779	323.0	51.2	126.3	3	Doc2013d[b]
84979		±7.67	±0.39	±0.023	±0.0106	±4.2	±5.0	±8.1		
17575−5740	TOK 55 Ba,Bb	8.92	2015.16	0.387	0.1225	345.7	342.3	104.1	2	New
87914		±0.36	±0.13	±0.020	±0.0026	±1.3	±8.7	±0.8		
17584+0428	KUI 84	14.715	2001.496	0.496	0.1746	351.5	190.0	62.8	1	Doc2005f
87991		±0.040	±0.051	±0.008	±0.0014	±0.8	±1.8	±1.2		
18092−2211	RST 3157	10.685	2015.031	0.409	0.1575	232.4	55.5	50.2	2	Tok2015c
88932		±0.045	±0.020	±0.008	±0.0019	±1.3	±1.3	±1.2		
18150−5018	I 429	63.10	2021.4	0.84	0.150	132.6	228.2	84.0	4	New
...		±5.75	±3.7	±0.16	±0.031	±2.9	±14.0	±2.1		
18368−2617	RST 3187 AB	18.37	2017.30	0.364	0.1661	40.6	7.2	70.1	3	New
91253		±0.18	±0.16	±0.022	±0.0020	±0.9	±2.9	±0.8		
18480−1009	HDS 2665	31.212	2020.007	0.705	0.4535	192.8	44.2	49.1	3	New
92250		±0.003	±0.194	±0.014	±0.0178	±1.3	±3.4	±3.4		
19581−4808	HDS 2842	35.28	2016.036	0.738	0.2364	254.2	60.6	70.2	3	Tok2015c
98274		±2.48	±0.065	±0.037	±0.0140	±2.4	±4.1	±2.2		
20057−3743	HDS 2865	50.0	2018.71	0.328	0.1778	4.2	131.7	131.5	4	New[a]
98979		fixed	±0.56	±0.040	±0.0043	±3.7	±6.6	±4.2		
20104−1923	HDS 2873	90.0	2007.46	0.484	0.3843	35.2	-0.3	94.0	5	New
99391		fixed	±0.67	±0.006	±0.0087	±0.9	±4.3	±0.4		
20202−3435	I 1416	20.16	2000.19	0.90	0.163	140.1	37.2	113.9	3	B_1961d
100266		±0.31	±1.24	fixed	±0.035	±3.2	±19.7	±11.6		
20217−3637	HDS 2908	12.74	2007.44	0.518	0.1120	107.8	338.9	80.8	3	New
100417		±0.24	±0.52	±0.046	±0.0065	±0.6	±10.7	±2.7		
20248−1943	HDS 2919	65.0	2020.90	0.474	0.3243	269.7	311.6	60.9	5	New[a]
100685		fixed	±0.75	±0.062	±0.0086	±2.9	±3.6	±2.5		
21073−5702	HDS 3009	54.08	2013.30	0.311	0.3482	350.1	143.3	56.8	3	New
104256		±4.21	±0.75	±0.030	±0.0050	±1.0	±8.3	±1.9		
22116−3428	CHR 230 Aa,Ab	66.5	2010.37	0.929	0.1156	318.7	305.0	70.5	3	New
109561		±11.0	±0.39	±0.024	±0.0168	±3.5	±7.5	±4.1		

References. — B_1961d — van den Bos (1961); Baz1989a — Baize (1989); Doc2005f — Docobo & Ling (2005); Doc2013d — Docobo & Andrade (2013); Hei1981a — Heintz (1981); Hei1992b – Heintz & Cantor (1992); Hei1996a — Heintz (1996); Hei1997 — Heintz (1997); Hor2011b — Horch et al. (2011); Hrt2011d — Hartkopf & Mason (2011); Koh2002 — Koehler & Petr-Gotzens (2002); Ole2004b — Olevic & Cvetkovic (2004); Tok2014a — Tokovinin et al. (2014); Tok2015c — Tokovinin et al. (2015); Zir2014a — Zirm (2014);

[a] Insufficient coverage.

[b] See Figure 1.

Table 2
Observations and residuals (Fragment)

WDS	T (yr)	θ (°)	ρ ($''$)	σ ($''$)	O−C$_\theta$ (°)	O−C$_\rho$ ($''$)
04180-3826	1991.2500	230.0	0.1360	0.0100	0.1	−0.0002
04180-3826	2014.0430	228.6	0.1332	0.0015	0.3	0.0003
04180-3826	2014.8536	207.0	0.1022	9.0047	−4.5	0.0051
04180-3826	2015.1053	201.1	0.0826	0.0020	−1.8	−0.0006
04180-3826	2015.7385	165.3	0.0566	0.0020	1.9	0.0001
04180-3826	2015.9080	148.8	0.0559	0.0020	0.6	0.0008
04180-3826	2016.1373	127.1	0.0578	0.0020	−1.3	−0.0010

Table 3
Parallaxes and photometry

WDS	HIP	Spectral Type	$\pi_{\rm HIP2}$ (mas)	$\pi_{\rm dyn}$ (mas)	$\mathcal{M}_1$ ($\mathcal{M}_\odot$)	$\mathcal{M}_2$ ($\mathcal{M}_\odot$)	V (mag)	$V-I_C$ (mag)	Δy (mag)	$\sigma_{\Delta y}$ (mag)	ΔI (mag)	$\sigma_{\Delta I}$ (mag)
04180−3826	20048	K2V	26.8	25.0	0.8	0.7	8.89	1.11	...	...	0.50	0.14
05229−4219	25148	G5V	15.1	15.1*	1.1	0.8	8.70	0.76	...	...	1.22	0.38
05542−2909	27901	F3V	18.5	17.2*	1.5	1.2	6.34	0.43	1.49	0.18	1.06	...
06018−7158	28573	K2/K3IV	15.0	15.6	0.9	0.8	9.77	1.09	...	...	0.60	0.12
06032+1922	28671	G0V	16.8	18.0	0.9	0.6	9.28	0.71	...	...	1.90	0.48
08369−7857	...	K4Ve	...	11.5	0.8	0.8	10.46	1.45	...	...	0.39	0.21
08398−6604	42496	K1V:	16.6	17.7*	0.9	0.7	9.73	0.97	1.93	0.73	1.51	0.34

Table 3 — *Continued*

WDS	HIP	Spectral Type	$\pi_{\rm HIP2}$ (mas)	$\pi_{\rm dyn}$ (mas)	$\mathcal{M}_1$ ($\mathcal{M}_\odot$)	$\mathcal{M}_2$ ($\mathcal{M}_\odot$)	V (mag)	$V-I_C$ (mag)	Δy (mag)	$\sigma_{\Delta y}$ (mag)	ΔI (mag)	$\sigma_{\Delta I}$ (mag)
08494+0341	43304	G5	28.2	29.7	1.0	0.5	7.96	0.79	...	...	2.94	0.52
09149+0427	45383	K0	55.7	46.4	0.8	0.5	7.91	1.19	3.98	...	2.13	0.46
09186+2049	45671	F5	9.2	9.1	1.3	1.1	8.64	0.51	...	...	0.77	...
09275−5806	46388	G2V	20.0	19.5*	1.2	1.1	7.20	0.67	0.73	0.34	...	...
09320−0111	46776	A3V	6.3	5.4*	3.6	3.3	4.54	0.16	0.44	0.16	...	...
09466−4955	47969	G5IV	6.8	6.9	1.4	1.2	8.73	0.83	0.99	0.10	1.23	0.17
09510−8004	48320	B8IV	3.9	6.3	2.4	1.6	6.47	0.12	2.05	0.14	1.69	0.18
10112−3245	49883	G1V	11.6	11.9	1.3	0.8	8.30	0.68	3.04	0.87	2.14	0.48
11102−1122	54580	G0	16.2	16.4*	1.1	1.1	7.70	0.72	0.30	0.14	0.22	0.19
11238−3829	55628	K1V	20.7	20.3*	0.9	0.9	8.51	0.83	0.37	0.17	0.39	0.46
11425+2355	57112	G5	21.9	23.3*	0.9	0.6	9.02	0.83	...	...	1.51	0.07
11525−1408	57894	G0V	15.6	17.5*	1.2	1.0	7.66	0.64	1.30	0.19	1.15	0.01
13072−5420	64025	G1/G2V	1.4	4.8	1.5	1.2	9.08	0.73	...	...	0.90	0.06
13081−7719	64091	K3V	23.3	26.1	0.9	0.6	8.76	1.01	...	...	1.79	0.07
13306−4238	65906	K4V	30.6	31.2	0.7	0.6	9.56	1.47	...	...	0.97	0.11
13377−2337	...	G5	...	12.3	0.9	0.7	10.17	0.80	2.10	...	0.25	...
13598−0333	68380	F8V	12.9	11.0*	1.8	1.5	6.36	0.56	1.13	0.12	0.93	...
14020−2108	68552	K0/K1V	20.0	22.1*	0.8	0.6	9.51	0.97	2.77	0.06	1.64	0.18
14383−4954	71577	A0IV	4.2	4.3*	2.7	2.2	6.51	0.05	0.98	0.20	...	...
14453−3609	72140	A1IV/V	4.8	5.1	2.1	1.6	7.37	0.12	1.44	0.23	...	...
14589+0636	73314	K0?	23.2	25.5*	0.9	0.8	8.45	0.88	0.69	0.12	0.56	0.11
15035−4035	73667	F3V	6.1	5.7	1.4	1.3	8.82	0.54	0.61	...	0.44	...
15042−1530	73724	F5/F6V	8.4	7.9	1.5	1.2	8.03	0.60	1.15	0.51	...	...
15251−2340	75478	G2V	15.3	15.5	1.0	1.0	8.48	0.65	0.52	0.36	0.28	0.14
15282−0921	75718	K2V	48.6	51.4*	0.9	0.6	6.89	0.86	3.40	0.04	2.21	0.24
15290−2852	75790	G0V	17.1	14.6	1.6	1.3	6.43	0.68	0.93	...	0.90	0.02
15317+0053	76031	G0	19.7	23.8*	1.1	0.9	7.42	0.71	1.56	0.43	1.25	0.15
15332−2429	76143	A7+k...	10.3	9.5*	2.0	1.4	6.26	0.38	1.75	0.17	1.18	0.02
15348−2808	76275	G8V	17.4	17.4	1.0	0.7	9.08	0.77	2.46	0.16	1.84	0.16
15548−6554	77921	G2V	21.0	22.1*	1.1	1.0	7.55	0.69	0.52	0.61	0.35	...
16544−3806	82709	G0V	15.6	17.3	1.1	0.7	8.40	0.69	3.27	0.15	2.32	...
17018−5108	83321	A7V	9.6	5.8	2.3	2.1	6.43	0.32	0.47	0.35	...	...
17066+0039	83716	K0V	17.3	18.4*	0.8	0.8	9.81	1.00	0.05	0.07	0.07	0.06
17221−7007	84979	B8/B9Vn...	2.5	2.6*	4.2	4.1	5.39	...	0.15	0.22	...	...
17575−5740	87914	K0V	25.1	24.9*	0.8	0.7	9.31	1.00	0.42	0.22	0.28	0.14
17584+0428	87991	K8	22.9	26.3*	0.7	0.6	9.80	1.40	1.16	...	0.48	...
18092−2211	88932	K3/K4V	30.5	28.2*	0.8	0.7	8.88	1.04	0.79	0.39	0.14	0.17
18150−5018	...	A0V	...	6.2	1.9	1.7	7.22	...	0.79	0.51	1.36	...
18368−2617	91253	G3V	21.5	18.7*	1.1	1.0	7.80	0.70	0.78	0.25	0.43	0.20
18480−1009	92250	K0	36.0	41.9*	0.8	0.5	8.45	0.93	3.65	...	2.18	0.02
19581−4808	98274	G0V	18.6	18.0*	1.1	0.8	8.35	0.68	2.28	0.62	1.68	0.18
20057−3743	98979	F3V	6.7	9.6	1.4	1.1	7.94	0.49	1.20	...	0.41	0.06
20104−1923	99391	G0V	16.4	14.6	1.4	0.8	7.28	0.65	3.09	0.38	2.29	0.17
20202−3435	100266	F8V	16.1	15.9*	1.5	1.2	6.62	0.66	1.24	0.09	1.10	0.02
20217−3637	100417	G0/G1V	16.8	15.4*	1.2	1.1	7.49	0.66	0.49	0.15	0.20	0.05
20248−1943	100685	K3V	18.3	17.0	0.9	0.8	9.40	0.98	...	...	0.68	0.11
21073−5702	104256	K1V	18.6	20.8*	0.9	0.7	8.82	0.84	2.33	0.13	1.58	0.05
22116−3428	109561	K1/K2III+..	4.2	4.2*	2.7	1.9	6.68	0.64	1.67	0.63	...	...